JOURNAL OF AGRICULTURAL AND FOOD CHEMISTRY

Article

pubs.acs.org/JAFC

Impact of High-Fat and High-Carbohydrate Diets on Liver Metabolism Studied in a Rat Model with a Systems Biology Approach

Hanne Christine Bertram,*[,†] Lotte Bach Larsen,[‡] Xiaoping Chen,[§,#] and Per Bendix Jeppesen[§]

[†]Department of Food Science, Aarhus University, Kirstinebjergvej 10, DK-5792 Aarslev, Denmark

[‡]Department of Food Science, Aarhus University, P.O. Box 50, DK-8830 Tjele, Denmark

[§]Department of Endocrinology MEA, Aarhus University Hospital, Aarhus University, DK-8000 Aarhus C, Denmark

[#]Department of Endocrinology, China−Japan Friendship Hospital, Beijing 100029, China

ABSTRACT: The aim of the present study was to investigate the use of an integrated metabolomics and proteomics approach in the elucidation of diet-induced effects on hepatic metabolism in a rat model. Nuclear magnetic resonance (NMR)-based metabolomics of liver extracts revealed a pronounced effect of a high-fat diet on the hepatic betaine content, whereas a carbohydrate-rich diet induced increases in hepatic glucose. In addition, the metabolomic investigations revealed that the high-fat diet was associated with increased hepatic lipid levels, which was not evident with the carbohydrate-rich diet. The proteomic investigations revealed strong high-fat diet effects on the expression of 186 proteins in the liver including malate dehydrogenase. Comparison of malate dehydrogenase expression determined by proteomics and NMR metabolite profiles revealed correlations between malate dehydrogenase and lactate, glucose, and glutamine/glutamate signals, thereby demonstrating a diet-induced regulation that was evident at both proteomic and metabolomic levels.

KEYWORDS: *hepatic metabolism, protein expression, metabonomics, proteomics, betaine, metabolic syndrome*

INTRODUCTION

Metabolomic approaches, which aim at characterizing a complete set of metabolites, have become widely used in intervention studies to study the impact of dietary and beverage components[1−6] and other types of studies related to nutrition and diet-related metabolic diseases.[7,8] In these types of studies, biofluids are analyzed to examine how the factor under investigation causes changes in the metabolite profile of blood or urine. Although these applications make it possible to follow the progression over time[9,10] and potentially identify dietary biomarkers,[11,12] the results do not provide direct information about the mechanisms responsible for these biofluid changes. In contrast, the liver has a range of metabolic functions and plays an important role in metabolism, and disturbances in the liver are likely to be a fundamental factor in both the initiation and progression of metabolic diseases.[13] Consequently, tissue-targeted metabolomic characterization of the liver can be expected to provide useful information about the mechanisms involved in the development of metabolic diseases as a function of diet, as has been demonstrated in liver samples from hypercholesterolemic pigs[14] and in different rodent models.[15−19]

Proteomics, which in analogy to metabolomics aims at describing the complete set of proteins present in a biological sample, is also an important tool for elucidating the cellular response to various treatments including dietary factors.[20,21] Furthermore, the use of proteomics for elucidating diet-induced changes in the heart of prediabetic mice has recently been demonstrated.[22] Linking information obtained from liver-specific metabolomics with liver-specific proteomics would pave the way for obtaining a better understanding of the primary pathways in the liver playing a key role in both the initiation and progression of metabolic diseases. Consequently, the aim of the present study was to investigate the impact of a high-fat/high-cholesterol diet or a high-carbohydrate diet on the liver metabolome and liver proteome by using a rat model in a systems biology approach. To the authors' knowledge, the present study is the first to apply a systems biology approach consisting of metabolomics and proteomic technologies to investigate diet-induced changes in hepatic metabolism and thereby obtain a better understanding of the molecular mechanisms related to intake of metabolic syndrome high-risk diets.

MATERIALS AND METHODS

Chemicals. Deuterium oxide (D, 99.9%) and chloroform-*d* (D, 99.8%) were purchased from Cambridge Isotope Laboratories, Inc. (Andover, MA). Urea ACS was purchased from Merck (Darmstadt, Germany). Thiourea (99% extra pure) was purchased from Acros Organics (Geel, Belgium), 3-[(cholamidopropyl)dimethylammonio]-1-propanesulfonate (CHAPS) (98%) was purchased from Calbiochem (Darmstadt, Germany), dithioerythritol (DTE) (99%) was purchased from Sigma-Aldrich (Taufkirchen, Germany), Phamalyte 3−10 was purchased from GE-Healthcare (Uppsala, Sweden), and BCA Protein Assay kit for determination of protein concentration was purchased from Pierce (Rockford, IL).

Animals and Sampling. Thirty-three male Wistar rats (Taconic, Ry, Denmark), all 6 weeks of age and having a body weight of about 230 g, were used. The rats were randomly divided into three groups with 11 in each and fed with three different diets. Group 1 was fed standard chow diet (Altromin 1324, Brogaarden, Denmark), group 2 a

Received: October 1, 2011
Revised: December 5, 2011
Accepted: December 19, 2011
Published: December 19, 2011

high fat containing diet (1.63% cholesterol, 0.41% cholic acid, 16.30% sunflower oil, and 81.66% chow diet) (Brogaarden, Denmark), and roup 3 was fed a high-carbohydrate diet (5.0% corn oil, 65.0% saccharose, and 30.0% chow diet) (Brogaarden, Denmark). The food intake and body weight were measured every second week throughout the study. The composition of the standard chow diet dry matter was 24% protein, 71% carbohydrate, and 5% lipids. No deaths were observed for groups 1 and 3, whereas two deaths occurred in group 2 on the high-fat diet due to diseases such as atherosclerosis and stroke. A 12 h light/dark cycle was used. After 20 weeks of intervention, the animals were fasted for 12 h before intraperitoneal injection of an overdose of sodium pentobarbital and killed by exsanguination. Liver samples were collected and immediately frozen in liquid nitrogen and subsequently stored at −80 °C, and eight liver samples from each treatment group were randomly selected for NMR and proteomics analyses. The experiment was carried out in accordance with the guidelines and approval of the Danish Council for Animal Experiments (no. 2010/561-1805).

Extraction for NMR and Proteomic Analyses. Rat liver samples were extracted using a method described by Atherton et al.[23] after slight modification. In brief, liver samples (about 100 mg) were homogenized for 1 min in ice-cold methanol/chloroform (2:1, v/v, 3 mL) using a Heidolph Diax 600 homogenizer (Schwabach, Germany). Samples were then sonicated for 30 min and, after the addition of 1 mL of ice-cold water and 1 mL of ice-cold chloroform, the samples were vortexed for 1 min and centrifuged at 4000*g* for 20 min (to allow phase separation). The aqueous supernatant (polar phase) was then collected, dried using an evacuated centrifuge (Savant, SVC 100H, Savant Instruments Inc., Hicksville, NY), and the organic phase was dried by using a nitrogen evaporator.

^{1}H NMR Spectroscopy. Prior to NMR analyses, water-soluble extracts were dissolved in D_2O containing sodium trimethylsilyl-[2,2,3,3-$^2H_4$]-1-propionate (TMSP) added as an internal standard, and lipid extracts were dissolved in chloroform-*d* containing tetramethylsilane (TMS). The NMR measurements were performed at 298 K on a Bruker Avance III 600 spectrometer, operating at a ^{1}H frequency of 600.13 MHz and equipped with a 5 mm ^{1}H TXI probe (Bruker BioSpin, Rheinstetten, Germany). ^{1}H NMR spectra of both water-soluble extracts and lipid extracts were obtained using a single 90° pulse experiment. For the water-soluble extract, water suppression was achieved by irradiating the water peak during the relaxation delay of 5 s. A total of 128 transients of 16K data points spanning a spectral width 12.15 ppm were collected. Spectra were baseline-corrected and referenced to the TMSP or TMS signal at 0 ppm.

The ^{1}H NMR spectra obtained on water-soluble metabolites were divided into 0.007 ppm integral regions and integrated in the region 0.5−10.0 ppm. Before further data analysis, the spectral region containing signals from residual water (4.7−5.0 ppm) was removed. The reduced spectra consisting of 1190 independent variables were normalized to the whole spectrum to remove any concentration effects. The ^{1}H NMR spectra obtained on the chloroform phase were likewise subdivided into 0.007 ppm integral regions and integrated in the region 0.3−6.0 ppm, and the reduced spectra consisting of 743 independent variables were normalized to the TSP signal.

Two-Dimensional Gel Electrophoresis (2-DGE). Eight biological replicates of liver homogenates of each treatment (high fat, high carbohydrate, and controls) were used for 2-DGE-based proteomic analysis and analyzed in a single gel set, giving a total of 24 gels analyzed. The stored liver homogenates were thawed, and 300 μL of lysis buffer (6 M urea, 2 M thiourea, 1.5% (w/v) Pharmalyte, 0.8% (w/v) CHAPS, 1% (w/v) DTE (in water)) was added to each sample. After incubation for 30 min at room temperature, the samples were homogenized and further incubated for 2 h at room temperature under shaking. After centrifugation at 6000*g* for 20 min at 4 °C, the protein concentrations of the supernatants were determined by the bicinchoninic acid (BCA) assay (Bio-Rad). A volume of each sample corresponding to 120 μg of protein was applied to each gel. 2-DGE was carried out essentially as described earlier,[24] using 11 cm IPG strips (pH 5−8) for the first dimension and 12.5% Criterion gels (Bio-Rad) for the second dimension. The gels were stained with the fluorescent stain Flamingo Pink (Bio-Rad) according to the instructions of the manufacturer and scanned using a Molecular Imager FX (Bio-Rad, Hercules, CA) using excitation at 512 nm and emission detected at 535 nm. Prior to excision of spots for mass spectrometry (MS), the gels were restained with colloid Coomassie Blue R-250.[25]

Image Analysis of 2-D Gels. Gel spots on the gel scans were detected and quantified using PDQuest imaging software (Bio-Rad). After initial analysis using automated spot detection and segmentation, all images were manually checked, and the spots were matched by comparing the relative positions of the individual spots on each gel, which reduced the number of spots used in the further analysis. The spots were quantified by adding the pixel intensities within the spot boundary, and the spot volumes were calculated. To overcome gel-to-gel variations in spot intensities due to technical variations related to the staining procedure, etc., the relative spot volumes were calculated for each separate spot on the gels, and these values were used in the further data analysis.

Identification of Liver Proteins by MALDI-TOF MS. Protein spots of significance were subjected to in-gel digestion for peptide mass fingerprinting (PMF) by the addition of trypsin. For mass spectrometric analysis the resulting peptides were desalted, concentrated, and eluted in 0.5 μL of matrix solution (15−20 g/L of α-cyano-4-hydroxycinnamic acid in 70% acetonitrile) directly onto the MALDI target plate as described earlier.[24] Mass spectra were obtained using a Bruker Ultraflex MALDI-TOF tandem mass spectrometer in reflection mode.[24] A peptide calibration standard (0.2 μL) containing seven standard peptides ranging in molecular mass from 1046.54 to 3147.47 Da was spotted separately onto the MALDI target plate. Liver proteins were identified by PMF by mass searches in the database SwissProt (Swiss Institute of Bioinformatics, Genève, Switzerland) using the search program Mascot (Matrix Science, Boston, MA). In this program the experimental mass value, obtained from MS, is compared with calculated peptide masses from a database. A scoring algorithm is used to identify the closest match. Significant protein identifications (protein scores above 60, $p < 0.05$) were reported and manually verified.

Statistical Analyses. Multivariate data analysis was performed using the Unscrambler software version 9.2 (Camo, Oslo, Norway). Principal component analysis (PCA) was applied to the centered data to explore any clustering behavior of the samples. In addition, partial least-squares (PLS) regression was performed with the NMR variables as *X*- and proteomic spots as *Y*-variables. During PLS regressions, Martens' uncertainty test[26] was used to eliminate noisy variables. All models were validated by full cross-validation.

For the proteomic data, statistical analysis was carried out by comparing relative spot volumes obtained from the eight gels obtained for treated animals (high fat or high carbohydrate) with those for the eight controls using unpaired two-tailed *t* test with 95% confidence interval. Data were calculated as mean relative spot volumes ± standard error of the mean (SEM). Fold change in mean relative spot volumes was calculated relative to the control. For the body weight and food intake a one-way ANOVA test was used to test significant differences at the same time points during the intervention period. A *p* value of <0.05 was considered to be significant.

RESULTS

Body Weight and Food Intake. At the beginning of the intervention study no significant difference was observed in body weight between the Wistar control rats and the rats fed high-carbohydrate or high-fat diets (Figure 1). However, from week 2 a significant weight reduction (19%) was observed in rats fed the high-carbohydrate diet compared to the control diet, and this weight reduction lasted for the rest of the intervention periodm where a reduction of up to 51% was seen ($p < 0.01$). The high-fat diet caused a significant reduction in body weight after 14 weeks of intervention, when a reduction of

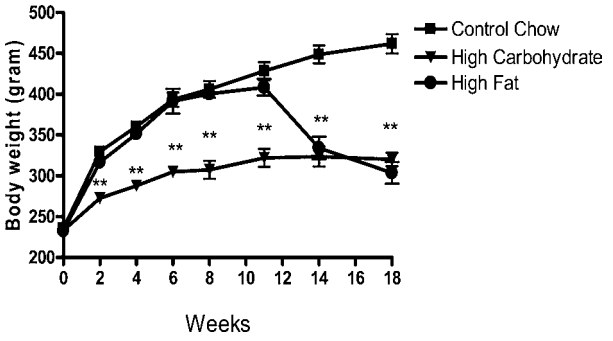

Figure 1. Development in body weight of the experimental Wistar rats during the 18 week intervention period. The observed weight loss at week 14 in the high-fat group is due to the development of severe type 2 diabetes, which is not seen in the other two groups. Presented data are mean values ± SEM (n = 11 in each group, ** = $p < 0.01$ denotes significant difference from the control).

approximately 51% was seen compared to the control diet ($p < 0.01$) (Figure 1).

The food intake was measured every second week throughout the study (Figure 2). No significant differences in

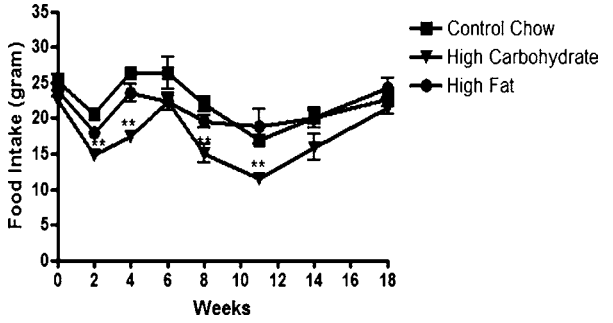

Figure 2. Food intake for the experimental wistar rats during the 18 week intervention period. Presented data are mean values ± SEM (n = 11 in each group, ** = $p < 0.01$ denotes significant difference from the control).

food intake were observed between the high-fat group and the control group. However, a reduced food intake was seen for the high-carbohydrate group compared to the control group; the food intake was reduced from 41 to 53% ($p < 0.01$) (Figure 2).

Rats exposed to either high fat or high carbohydrate in the diet were characterized by changes in their metabolic and proteomic fingerprints by NMR and 2-D gel-based proteomics, respectively.

NMR Metabolic Profiling. Figure 3 shows representative ^{1}H NMR spectra obtained on aqueous and organic liver extracts. Several signals are observed, which have been assigned on the basis of existing literature.[27−29] PCA on the NMR spectra obtained on water-soluble extracts revealed a clear grouping of the samples into the different diet groups along the first principal component (Figure 4A,C). Analysis of the first loading reveals that the separation into control and high-fat samples can mainly be ascribed to signals from betaine at 3.26 ppm ($N(CH_3)_3$ protons) and 3.90 ppm (CH_2 protons) together with a signal from lactate at 1.32 ppm (CH_3 protons), which all have higher intensities in liver samples from rats fed a high-fat diet compared with rats fed a standard chow diet (Figure 4B). The separation of samples into control and high-carbohydrate samples mainly can be ascribed to signals arising

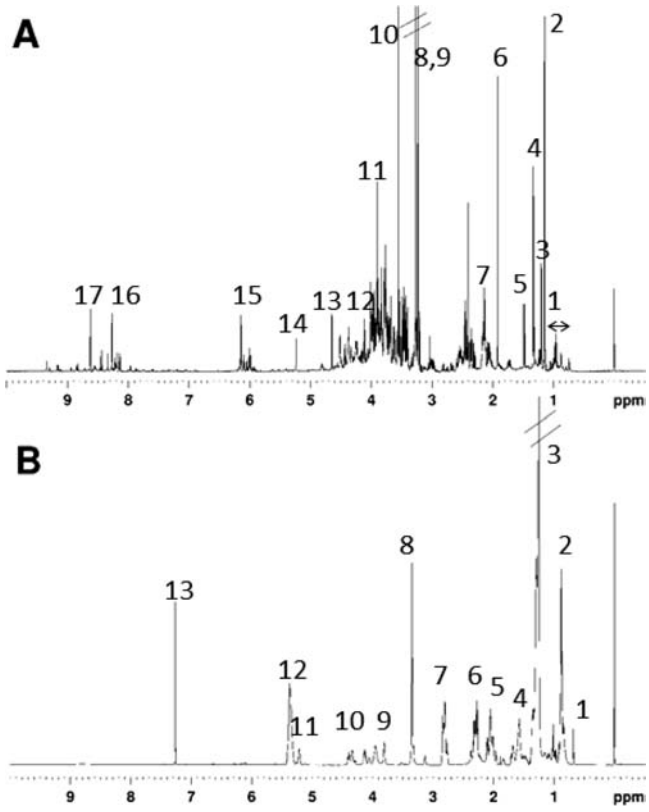

Figure 3. Representative 600 MHz ^{1}H NMR spectra obtained on dual methanol/chloroform extracts of rat liver samples: (A) aqueous extract; (B) organic extract. Assignments in (A): 1, branched-chain amino acids; 2, isobutyrate; 3, β-hydroxybutyrate; 4, lactate; 5, alanine; 6, acetate; 7, methionine; 8, choline; 9, betaine/trimethylamine-N-oxide; 10, glycine; 11, betaine; 12, lactate; 13, β-glucose; 14, α-glucose; 15, inosine/adenosine and nucleotides; 16, nucleotides; 17, nucleotides. Assignments in (B): 1, cholesterol CH_3; 2, lipid CH_3; 3, lipid CH_2; 4, lipid CH_2CH_2CO; 5, lipid $CH_2C{=}C$; 6, lipid CH_2CO; 7, $C{=}CCH_2C{=}C$; 8, lipid $N(CH_3)_3$; 9, lipid $CH_2OPO_2^-$; 10, lipid CH_2OCOR; 11, lipid CH_2OCOR; 12, lipid $CH{=}CH$; 13, residual chloroform.

from glucose, the anomeric CH1 from α-glucose at 5.24 ppm, the anomeric CH1 from β-glucose at 4.64 ppm, and several signals in the ∼3−4 ppm region originating from various CH protons, which all have lower intensities in control samples compared with samples from rats fed a high-carbohydrate diet (Figure 4D). In addition, a signal from lactate at 1.32 ppm has lower intensity in control samples compared with samples from rats fed a high-carbohydrate diet, whereas signals from aromatic compounds (∼7−9 ppm) have higher intensities in control samples compared with samples from rats fed a high-carbohydrate diet (Figure 4D).

PCA on the NMR spectra obtained on the chloroform phase revealed also strong clustering of the control and high-fat samples (Figure 5A). Analysis of the loading reveals contributions from multiple signals, which can be ascribed to an overall higher lipid content in liver samples from rats fed a high-fat diet compared with liver samples from rats fed a standard chow diet (Figure 5B). PCA on NMR spectra obtained on the chloroform phase from control and high-carbohydrate samples revealed no obvious grouping of these two treatment groups (Figure 5C).

Proteomic Profiling. After a manual check of the automatically assigned number of spots, a total of 516 protein

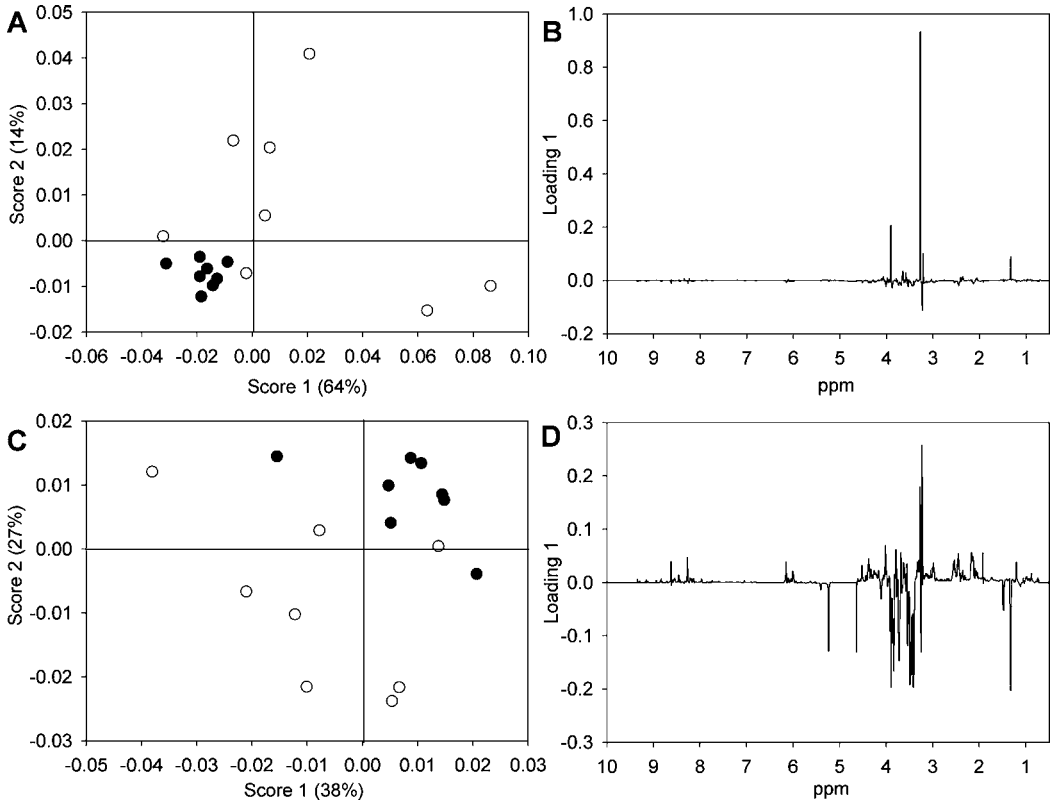

Figure 4. (A) PCA score plot showing the two first principal components for aqueous NMR spectra obtained on liver samples from rats fed control (solid circles) and high-fat (open circles) diets. (B) Corresponding loading plot of the first principal component. (C) PCA score plot showing the two first principal components for aqueous NMR spectra obtained on liver samples from rats fed control (solid circles) and high-carbohydrate (open circles) diets. (D) Corresponding loading plot of the first principal component.

spots were annotated by image analysis and used in the further statistical analysis. The proteomic signature of liver proteins in response to the dietary treatments, high fat or high carbohydrate, was analyzed by 2-DGE (Figure 6), and the significance of the spots was further tested by statistical *t* test of relative spot volumes. Of the 516 annotated proteins, 186 protein spots for high fat and 35 for high carbohydrate were found to be differentially expressed ($p < 0.05$) when compared with the control. PCA of the proteomic data confirmed that the changes in the proteomic profiles of the liver biopsies in response to high fat were larger than those observed for the high-carbohydrate diet, which mainly grouped together with the control (data not shown). This confirmed that the proteomic signatures of the liver samples overall were more affected by the high-fat diet than by the high-carbohydrate diet, and the further study of relationship between metabolic and proteomic data therefore focused on the data obtained by the high-fat diet treatment.

Relationship between Metabolic and Proteomic Profiles. To investigate the relationship between the metabolic profiles and significant proteomic spots, PLS regressions were carried out between the aqueous NMR spectra (*x*-data) and each of the 186 proteomic spots identified to be significantly different between high-fat liver samples and control samples (*y*-data). For a total of 11 spots, a correlation coefficient $R^2 > 0.8$ was obtained. MALDI-TOF MS was carried out to identify these 11 spots that correlated with NMR metabolite profiles. Of the 11 spots, 9 spots were identified by PMF (Figure 6; Table 1), whereas the remaining 2 spots could not be identified. The loadings from the PLS regressions between NMR metabolite profiles and the nine identified proteomic spots are shown in Figure 7. In general, several regions in the NMR spectra were correlated with the 9 spots. These regions included signals in the aromatic regions (~8.3−8.6 ppm) that probably represent nucleotides, and which were correlated with the proteomic spots identified as cytochrome *b*-c1, annexin, 60 kDa heat-shock protein, malate dehydrogenase, flavin reductase, keratin, and protein DJ. Signals at ~2.12 and ~2.45 ppm that probably represent glutamine/glutamate were also present in several loadings including loadings for cytochrome *b*-c1, annexin, 60 kDa heat-shock protein, malate dehydrogenase, flavin reductase, keratin, and protein DJ-1. In addition, the anomeric glucose signals at 4.64 and 5.23 ppm appeared in the loadings for cytochrome *b*-c1, malate dehydrogenase, and regucalcin. Finally, multiple signals in the ~3.0−4.0 ppm region representing various sugar and amino acid protons and multiple signals in the ~0.7−1.10 ppm region representing various branched-chain amino acids were present in several of the loading plots (Figure 7).

DISCUSSION

The present feasibility study demonstrated how metabolomics and proteomics may be integrated in the study of diet-induced effect on hepatic metabolism. Thus, the effects of a high-fat diet and a carbohydrate-rich diet on the liver metabolome and the liver proteome were investigated in a rat model. Body weight and food intake registrations revealed that the fat diet resulted in an unusual body weight loss after 14 weeks of intervention, probably due to the development of severe insulin resistance and cardiovascular-related symptoms, which are some of the

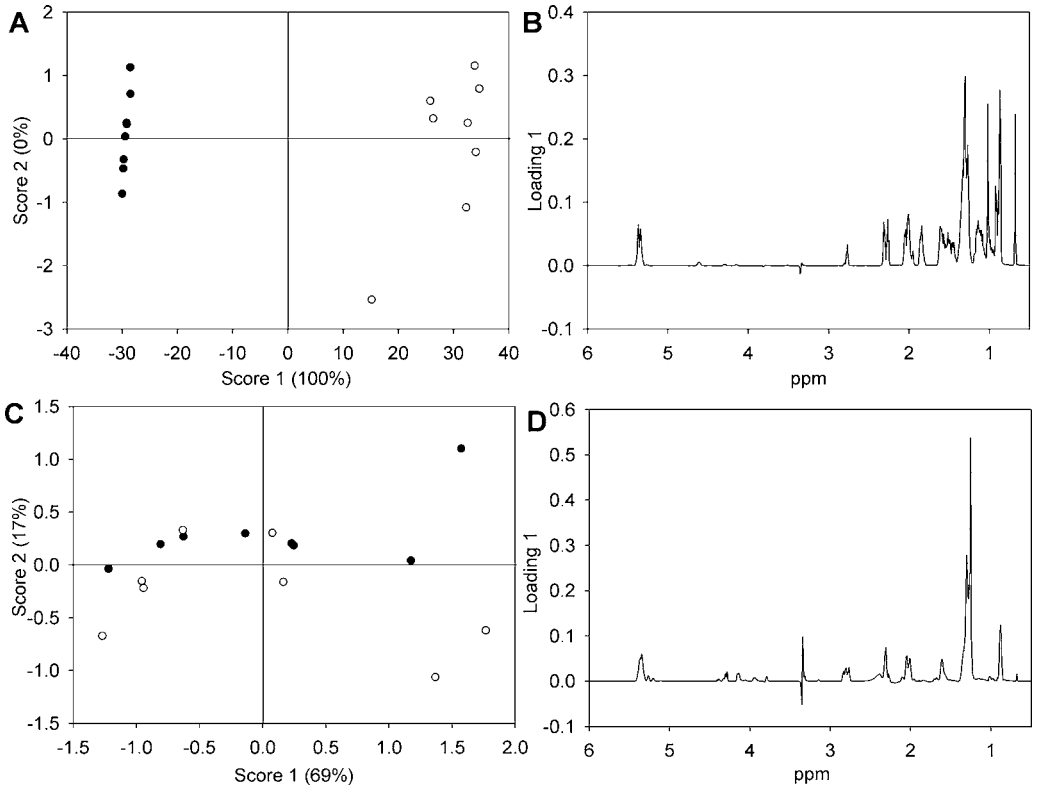

Figure 5. (A) PCA score plot showing the two first principal components for NMR spectra obtained on chloroform extracts of liver samples from rats fed control (solid circles) and high-fat (open circles) diets. (B) Corresponding loading plot of the first principal component. (C) PCA score plot showing the two first principal components for NMR spectra obtained on chloroform extracts of liver samples from rats fed control (solid circles) and high-carbohydrate (open circles) diets. (D) Corresponding loading plot of the first principal component.

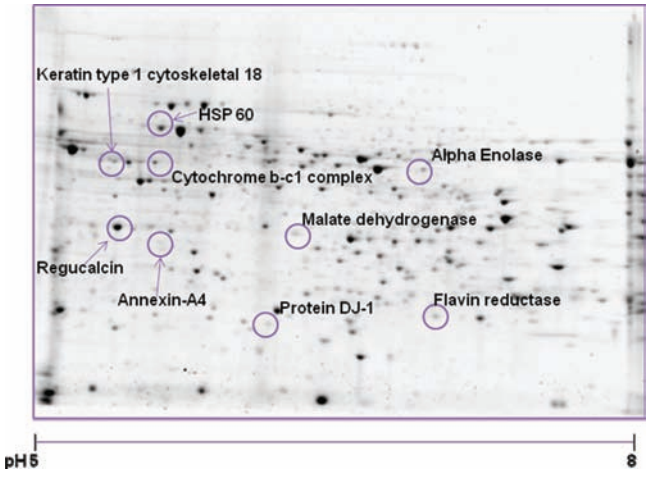

Figure 6. Proteomic profile of liver biopsies after treatment with high fat as analyzed by 2-DGE visualized by fluorescence staining. The positions of identified protein spots with high correlations to NMR data by PLSR ($R^2 > 0.8$) are indicated.

Table 1. Results from Identification of Proteomic Spots by MALDI TOF MS and PLS Regressions ($n = 24$) between the NMR Metabolite Profile and the Proteomic Data for a High-Fat Diet

identified protein	P value (t test)	mean (fold) F/C[a]	R value obtained from PLS regression	score[b]	Uniprot accession no.
regucalcin	0.02	1.2	0.83	105	Q03336
keratin type 1 cytoskeletal 18	0.00025	2.1	0.83	185	Q5BJY9
cytochrome *b*-c1 complex subunit 1	0.0120	1.5	0.91	105	Q68FY0
annexin-A4	0.0010	2.0	0.94	114	P55260
60 kDa heat shock protein	0.024	0.7	0.90	148	P63038
protein DJ-1 (contraception-associated protein 1)	0.0040	0.4	0.80	105	O88767
malate dehydrogenase	0.00027	0.5	0.86	67	P14152
flavin reductase	0.00086	0.6	0.88	95	Q923D2
α-enolase	4.5×10^{-5}	0.5	0.84	123	P04764

[a]Fold change in spot volumes relative to the control. [b]All protein identification scores in the Mascot search were significant.

criteria defining the metabolic syndrome. Knowledge regarding weight loss at high carbohydrate intake is still being discussed at a hypothetical level. Studies have shown that subjects consuming an ad libitum low-fat diet generally experience a reduction in fat mass without increased hunger.[30−33] A possible explanation is that dietary fat restriction produces weight loss by increasing CNS sensitivity to leptin, allowing energy intake, adipose mass, and leptin levels to fall without a compensatory increase in appetite. This explanation is supported by animal experiments showing that high-fat diets promote leptin resistance and that a reduction of dietary fat intake restores normal leptin action in the CNS, which may explain the observed weight loss.[34−37] An alternative explanation is that dietary fat restriction produces weight loss by increasing

dx.doi.org/10.1021/jf203994k | J. Agric.Food Chem. 2012, 60, 676−684

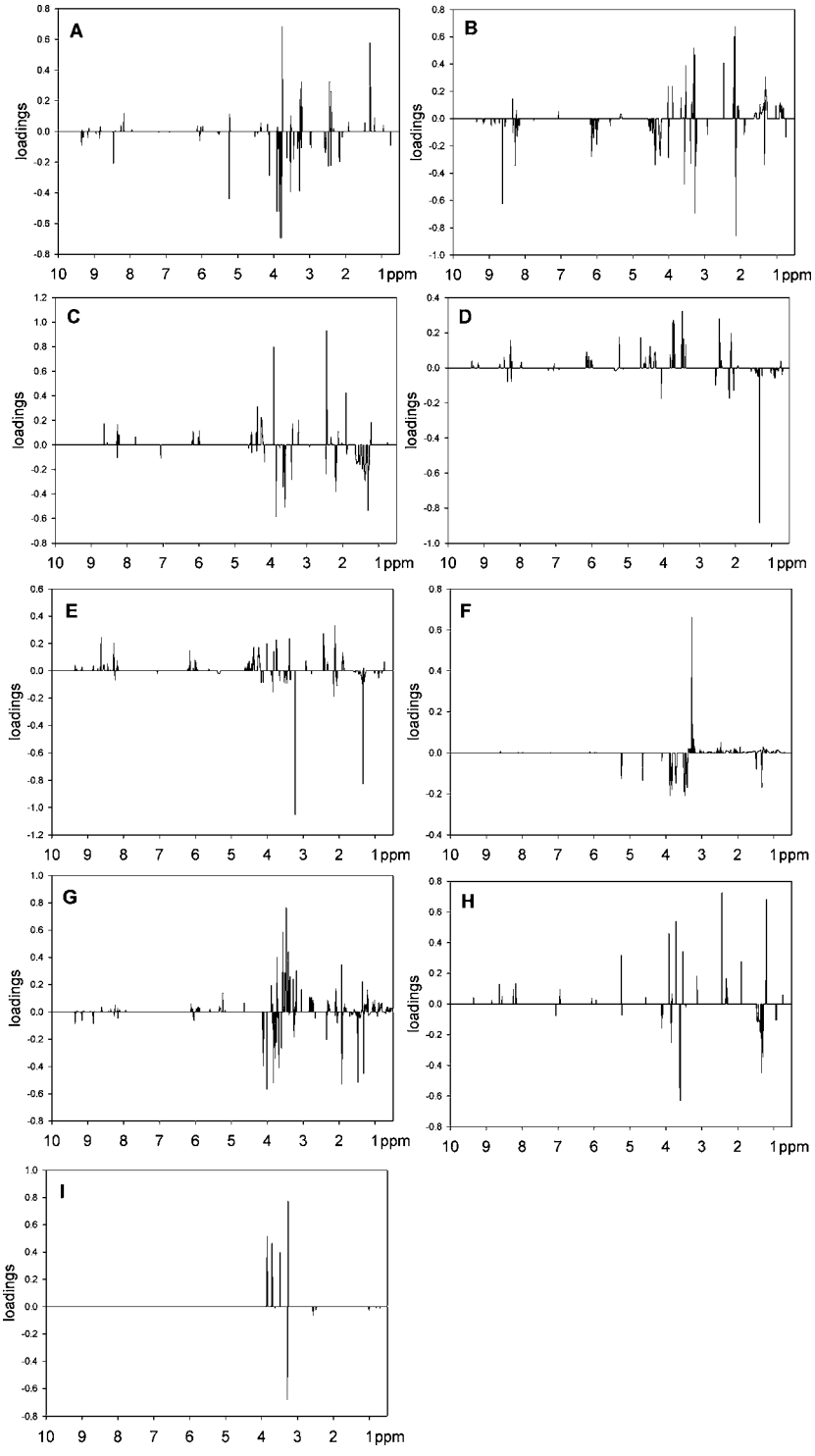

Figure 7. Loading weights obtained from PLS regressions with NMR variables as *X* and proteomic spots: (A) cytochrome *b*-c1; (B) annexin-A4; (C) 60 kDa heat shock protein; (D) malate dehydrogenase; (E) flavin reductase; (F) regucalcin; (G) keratin type 1; (H) protein DJ-1; (I) α-enolase.

circulating leptin levels, thereby delivering a stronger satiety message to the CNS and reducing energy intake.[38]

NMR-based metabonomics revealed a strong impact of diet on the liver metabolite profile, and liver samples from normally fed control rats and rats fed either a high-fat diet or a carbohydrate-rich diet could clearly be discriminated. A strong effect of diet on the content of betaine was observed, which was increased in liver samples from rats fed a high-fat diet. This finding must be considered striking as betaine functions as the basis of the enzyme betaine/homocysteine methyltransferase. By assisting in the remethylation of homocysteine, betaine removes homocysteine to form methionine and maintain the *S*-adenosylmethionine level, and in this sense betaine is involved in homocysteine metabolism, which is recognized as a risk factor for cardiovascular disease. Noteworthy, an association between hyperhomocysteinemia and hyperlipidemia has been proposed,[39] and it has further been suggested that hypomethylation associated with hyperhomocysteinemia is respon-

dx.doi.org/10.1021/jf203994k | *J. Agric.Food Chem.* 2012, 60, 676–684

sible for increased hepatic biosynthesis and uptake of cholesterol and triglycerides and lipid accumulation in tissues.[39] The higher betaine content in the liver of rats fed high fat probably reflects a higher activity/turnover of the methionine/homocysteine cycle in these liver samples, and the present results are thereby in agreement with a connection between hyperlipidemia and hyperhomocysteinemia. However, further studies are needed to investigate why a high-fat diet caused a higher activity/turnover of the methionine/homocysteine cycle in contrast to a lower activity/turnover as recently suggested in a metabolomic study on liver samples from mice fed a high-fat diet.[19]

NMR-based metabolomics of liver samples from rats fed a carbohydrate-rich diet showed that these liver samples had a higher content of carbohydrates compared with rats fed a normal diet. Previous studies elucidating the effect of carbohydrate intake on hepatic glucose metabolism have shown that carbohydrate intake may affect hepatic glucose production by changing the rate of glycolysis.[40−42] Even though these studies have been concerned with carbohydrate restriction, a similar mechanism could be expected with high levels of carbohydrate, and consequently, this may explain the findings in the present study. In contrast to glycolysis, there are indications that gluconeogenesis remains relatively stable independent of metabolic conditions.[43] Furthermore, hepatic lactate, which is a gluconeogenic precursor, was also found to be elevated with a carbohydrate-rich diet in the present study.

The proteomic analysis also revealed a strong effect of diet on the liver protein profile. A total of 186 proteomic spots were identified to differ significantly in intensity between liver samples from rats fed a control diet and rats high fat diet. Consequently, a strong effect of diet on the expression of protein in liver was demonstrated in the present study. Identification of 186 spots is quite labor-intensive. In the present study we therefore carried out PLS regressions between the NMR liver metabolite profile and the 186 spots to select the most important proteomic spots, which resulted in 11 spots that were strongly correlated with the NMR liver metabolite profile. Nine of these proteomic spots were identified by MALDI TOF MS analysis (Table 1). Intriguingly, none of these were closely associated with betaine metabolism, which may be expected because a strong effect on liver betaine was observed in the NMR metabolite profile. Consequently, in the present study the combination of metabonomics and proteomics unraveled very diverse and complementary information in relation to effects of a high-fat diet on the liver. The nine proteomic spots found to be highly correlated with the NMR liver metabolite profiles presented a wide range of proteins, including both major liver proteins, such as regucalcin and HSP60, and minor proteins and enzymes including α-enolase, malate dehydrogenase, flavin reductase, and protein DJ-1. The positions of these listed proteins all corresponded well with the positions reported earlier for the reference map of the porcine hepatocyte proteome.[44] The fact that hepatic malate dehydrogenase was found to be affected by diet and correlated to the NMR metabolite profile is probably the most striking finding. Malate dehydrogenase catalyzes the conversion of malate into oxaloacetate in the citric acid cycle. Transamination of α-ketoglutarate, an intermediate in the citric acid cycle, gives glutamate, which may explain the correlation between malate dehydrogenase and glutamine/glutamate signals in the NMR spectra (Figure 7D). In addition, malate dehydrogenase is also involved in gluconeogenesis, in which lactate is an important precursor. Consequently, the present findings showing a correlation between hepatic malate dehydrogenase expression, hepatic lactate, glucose, and glutamine/glutamate levels are sound and reveal a diet-induced regulation that is evident at both the proteomic and metabolomic levels.

In addition to proteins related to energy metabolism, the proteomic spots found to be highly correlated with the NMR liver metabolite also included regucalcin, a protein regulating calcium signaling, a heat-shock protein, keratin, annexin, and protein DJ-1, which is a contraception-associated protein. These correlations remain unexplained. It should be noted that the fact that multivariate data analysis reveals a correlation between variables does not necessarily mean that there is a causal relationship. In contrast, correlations may be caused by confounding or indirect effects. Thus, it can be concluded that extraction of significant information from systems biology approaches, which contain a wealth of data, remains a challenge, and the success of such approaches relies to a great extent on the development of efficient techniques for data analysis and tools that enable linkage of biochemical pathways and different postgenomic levels.

AUTHOR INFORMATION

Corresponding Author

*Phone: (+45) 871 58 353. Fax: (+45) 89 99 34 94. E-mail: HanneC.Bertram@agrsci.dk.

Funding

The Danish Research Council FTP is thanked for financial support through the project "Advances in food quality and nutrition research through implementation of metabolomics technologies" (274-09-107).

REFERENCES

(1) Bertram, H. C.; Bach Knudsen, K. E.; Serena, A.; Malmendal, A.; Nielsen, N. C.; Fretté, X. C.; Andersen, H. J. NMR-based metabonomic studies reveal changes in the biochemical profile of plasma and urine from pigs fed high-fibre rye bread. *Br. J. Nutr.* **2006**, *95*, 955−962.

(2) Bertram, H. C.; Hoppe, C.; Petersen, B. O.; Duus, J. Ø.; Mølgaard, C.; Michaelsen, K. F. An NMR-based metabonomic investigation on effects of milk and meat protein diets given to 8-year-old boys. *Br. J. Nutr.* **2007**, *97*, 758−763.

(3) Yang, H. P.; Pang, W.; Lu, H.; Cheng, D. M.; Yan, X. Z.; Cheng, Y. Y.; Jiang, Y. G. Comparison of metabolic profiling of cyanidin-3-*O*-galactoside and extracts from blueberry in aged mice. *J. Agric. Food Chem.* **2011**, *59*, 2069−2076.

(4) Daykin, C. A.; Van Duynhoven, J. P. M.; Groenewegen, A.; Dachtler, M.; Van Amelsvoort, J. M. M.; Mulder, T. P. J. Nuclear magnetic resonance spectroscopic based studies of the metabolism of black tea polyphenols in humans. *J. Agric. Food Chem.* **2005**, *53*, 1428−1434.

(5) Bertram, H. C.; Jeppesen, P. B.; Hermansen, K. An NMR-based metabonomic investigation on effects of supplementation with isosteviol or soy protein to diabetic KKAy mice. *Diabetes, Obes. Metab.* **2009**, *11*, 992−995.

(6) Wang, Y. L.; Tang, H. R.; Nicholson, J. K.; Hylands, P. J.; Sampson, J.; Holmes, E. A metabonomic strategy for the detection of the metabolic effects of chamomile (*Matricaria recutita* L.). *J. Agric. Food Chem.* **2005**, *53*, 191−196.

(7) Lankinen, M.; Schwab, U.; Gopalacharyulu, P. V.; Seppanen-Laakso, T.; Yetukuri, L.; Sysi-Aho, M.; Kallio, P.; Suortti, T.; Laaksonen, D. E.; Gylling, H.; Poutanen, K.; Kolehmainen, M.; Oresic, M. Dietary carbohydrate modification alters serum metabolic

profiles in individuals with the metabolic syndrome. *Nutr. Metab. Cardiovasc. Dis.* **2010**, *20*, 249−257.
(8) Bertram, H. C.; Malmendal, A.; Nielsen, N. C.; Straadt, I. K.; Larsen, T.; Bach Knudsen, K. E.; Lærke, H. N. NMR-based metabonomics reveals that plasma betaine increases upon intake of high-fiber rye buns in hypercholesterolemic pigs. *Mol. Nutr. Food Res.* **2009**, *53*, 1055−1062.
(9) Zhang, Q.; Wang, G. J.; Jiye, A.; Ma, B.; Dua, Y.; Zhu, L. L.; Wu, D. Metabonomic profiling of diet-induced hyperlipidaemia in a rat model. *Biomarkers* **2010**, *15*, 205−216.
(10) Peters, S.; Janssen, H. G.; Vivo-Truyols, G. Trend analysis of time-series data: a novel method for untargeted metabolite discovery. *Anal. Chim. Acta* **2010**, *663*, 98−104.
(11) Pedersen, S. M. M.; Nielsen, N. C.; Andersen, H. J.; Olsson, J.; Simrén, M.; Öhman, L.; Svensson, U.; Malmendal, A.; Bertram, H. C. The serum metabolite response to diet intervention with probiotic acidified milk in irritable bowel syndrome patients is indistinguishable from that of non-probiotic acidified milk by ^{1}H NMR-based metabonomic analysis. *Nutrients* **2010**, *2*, 1141−1155.
(12) Heinzmann, S. S.; Brown, I. J.; Chan, Q.; Bictash, M.; Dumas, M. E.; Kochhar, S.; Stamler, J.; Holmes, E.; Elliott, P.; Nicholson, J K. Metabolic profiling strategy for discovery of nutritional biomarkers: proline betaine as a marker of citrus consumption. *Am. J. Clin. Nutr.* **2010**, *92*, 436−443.
(13) Stefan, N.; Kantartzis, K.; Häring, H.-U. Causes and metabolic consequences of fatty liver. *Endocrine Rev.* **2008**, *29*, 939−960.
(14) Bertram, H. C.; Duarte, I. F.; Gil, A. M.; Bach Knudsen, K. E.; Lærke, H. N. Metabolic profiling of liver from hypercholesterolemic pigs fed rye- or wheat-fibre breads and of liver from normal pigs fed a standard diet − a high-resolution magic angle spinning ^{1}H NMR spectroscopic study. *Anal. Chem.* **2007**, *79*, 168−175.
(15) Serkova, N. J.; Jackman, M.; Brown, J. L.; Liu, T.; Hirose, R.; Roberts, J. P.; Maher, J. J.; Niemann, C. U. Metabolic profiling of livers and blood from obese Zucker rats. *J. Hepatol.* **2006**, *44*, 956−962.
(16) van Ginneken, V.; Verhey, E.; Poelmann, R.; Ramakers, R.; van Dijk, K. W.; Ham, L.; Voshol, P.; Havekes, L.; Van Eck, M.; van der Greef, J. Metabolomics (liver and blood profi ling) in a mouse model in response to fasting: a study of hepatic steatosis. *Biochim. Biophys. Acta* **2007**, *1771*, 1263−1270.
(17) Gu, S. H.; Jiye, A.; Wang, G. J.; Zha, W. B.; Yan, B.; Zhang, Y.; Ren, H. C.; Cao, B.; Liu, L. S. Metabonomic profiling of liver metabolites by gas chromatography-mass spectrometry and its application to characterizing hyperlipidemia. *Biomed. Chromatogr.* **2010**, *24*, 245−252.
(18) Vinaixa, M.; Rodriguez, M. A.; Rull, A.; Beltran, R.; Blade, C.; Brezmes, J.; Canellas, N.; Joven, J.; Correig, X. Metabolomic assessment of the effect of dietary cholesterol in the progressive development of fatty liver disease. *J. Proteome Res.* **2010**, *9*, 2527−2538.
(19) Kim, H.-J.; Kim, J. H.; Noh, S.; Hur, H. J.; Sung, M. J.; Hwang, J.-T.; Park, J. H.; Yang, H. J.; Kim, M.-S.; Kwon, D. Y.; Yoon, S. H. Metabolomic analysis of livers and serum from high-fat diet induced obese mice. *J. Proteome Res.* **2011**, *10*, 722−731.
(20) de Roos, B. Proteomic analysis of human plasma and blood cells in nutritional studies: development of biomarkers to aid disease prevention. *Expert Rev. Proteomics* **2008**, *5*, 819−826.
(21) Kussmann, M.; Panchaud, A.; Affolter, M. Proteomics in nutrition: status quo and outlook for biomarkers and bioactives. *J. Proteome Res.* **2010**, *9*, 4876−4887.
(22) Cruz-Topete, D.; List, E. O.; Okada, S.; Kelder, B.; Kopchick, J. J. Proteomic changes in the heart of diet-induced pre-diabetic mice. *J. Proteomics* **2011**, *74*, 716−727.
(23) Young, J.; Larsen, L. B.; Malmendal, A.; Nielsen, N. C.; Straadt, I. K.; Oksbjerg, N.; Bertram, H. C. Creatine-induced activation of antioxidative defence in myotube cultures revealed by explorative NMR-based metabonomics and proteomics. *J. Int. Soc. Sports Nutr.* **2010**, *7*, 7−9.
(24) Atherton, H. J.; Bailey, N. J.; Zhang, W.; Taylor, J.; Major, H.; Shockcor, J.; Clarke, K.; Griffin, J. L. A combined ^{1}H-NMR spectroscopy- and mass spectrometry-based metabolomic study of the PPAR-α null mutant mouse defines profound systemic changes in metabolism linked to the metabolic syndrome. *Physiol. Genomics* **2006**, *27*, 178−186.
(25) Kang, D. H.; Gho, Y. S.; Suh, M. K.; Kang, C. H. Highly sensitive and fast protein detection with coomassie brilliant blue in sodium dodecyl sulfate-polyacrylamide gel electrophoresis. *Bull. Korean Chem. Soc.* **2002**, *23*, 1511−1512.
(26) Martens, H.; Martens, M. Modified jack-knife estimation of parameter uncertainty in bilinear modelling by partial least squares regression (PLSR). *Food Qual. Pref.* **2000**, *11*, 5−16.
(27) Lindon, J. C.; Nicholson, J. K.; Everett, J. R. NMR spectroscopy of biofluids. *Annu. Rep. NMR Spectrosc.* **1999**, *38*, 1−88.
(28) Wishart, D. S.; Knox, C.; Guo, A. C.; Eisner, R.; Young, N.; Gautam, B.; Hau, D. D.; Psychogios, N.; Dong, E.; Boutra, S.; Mandal, R.; Sinelnikov, I.; Xia, J.; Jia, L.; Cruz, J. A.; Lim, E.; Sobsey, C. A.; Shrivastava, S.; Huang, P.; Liu, P.; Fang, L.; Peng, J.; Fradette, R.; Cheng, D.; Tzur, D.; Clements, M.; Lewis, A.; De Souza, A.; Zuniga, A.; Dawe, M.; Xiong, Y.; Clive, D.; Greiner, R.; Nazyrova, A.; Shaykhutdinov, R.; Li, L.; Vogel, H. J.; Forsythe, I. HMDB: a knowledgebase for the human metabolome. *Nucleic Acids Res.* **2009**, *37* (Suppl. 1), D603−D610.
(29) Waters, N. J.; Holmes, E.; Waterfield, C. J.; Farrant, R. D.; Nicholson, J. K. NMR and pattern recognition studies on liver extract and intact livers from rats treated with α-naphthylisothiocynate. *Biochem. Pharmacol.* **2002**, *64*, 67−77.
(30) Schaefer, E. J.; Lichtenstein, A. H.; Lamon-Fava, S.; McNamara, J. R.; Schaefer, M. M.; Rasmussen, H.; Ordovas, J. M. Body weight and low-density lipoprotein cholesterol changes after consumption of a low-fat ad libitum diet. *JAMA, J. Am. Med. Assoc.* **1995**, *274*, 1450−1455.
(31) Siggaard, R.; Raben, A.; Astrup, A. Weight loss during 12 weeks' ad libitum carbohydrate-rich diet in overweight and normal-weight subjects at a Danish work site. *Obes. Res.* **1996**, *4*, 347−356.
(32) Astrup, A.; Grunwald, G. K.; Melanson, E. L.; Saris, W. H.; Hill, J. O. The role of low-fat diets in body weight control: a meta-analysis of ad libitum dietary intervention studies. *Int. J. Obes. Relat. Metab. Disord.* **2000**, *24*, 1545−1552.
(33) Kendall, A.; Levitsky, D. A.; Strupp, B. J.; Lissner, L. Weight loss on a low-fat diet: consequence of the imprecision of the control of food intake in humans. *Am. J. Clin. Nutr.* **1991**, *53*, 1124−1129.
(34) Lin, L.; Martin, R.; Schaffhauser, A. O.; York, D. A. Acute changes in the response to peripheral leptin with alteration in the diet composition. *Am. J. Physiol.* **2001**, *280*, R504−R509.
(35) Van Heek, M.; Compton, D. S.; France, C. F.; Tedesco, R. P.; Fawzi, A. B.; Graziano, M. P.; Sybertz, E. J.; Strader, C. D.; Davis, H. R. Jr. Diet-induced obese mice develop peripheral, but not central, resistance to leptin. *J. Clin. Invest.* **1997**, *99*, 385−390.
(36) El-Haschimi, K.; Pierroz, D. D.; Hileman, S. M.; Bjorbaek, C.; Flier, J. S. Two defects contribute to hypothalamic leptin resistance in mice with diet-induced obesity. *J. Clin. Invest.* **2000**, *105*, 1827−1832.
(37) Widdowson, P. S.; Upton, R.; Buckingham, R.; Arch, J.; Williams, G. Inhibition of food response to intracerebroventricular injection of leptin is attenuated in rats with diet-induced obesity. *Diabetes* **1997**, *46*, 1782−1785.
(38) Havel, P. J.; Townsend, R.; Chaump, L.; Teff, K. High-fat meals reduce 24-h circulating leptin concentrations in women. *Diabetes* **1999**, *48*, 334−341.
(39) Wang, H.; Tan, H.; Yang, F. Mechanisms in homocysteine-induced vascular disease. *Drug Discovery Today* **2005**, *2*, 25−31.
(40) Schwarz, J. M.; Neese, R. A.; Turner, S.; Dare, D.; Hellerstein, M. K. Short-term alterations in carbohydrate energy intake in humans. Striking effects on hepatic glucose production, de novo lipogenesis, liplysis, and whole-body fuel selection. *J. Clin. Invest.* **1995**, *96*, 2735−2743.
(41) Bisschop, P. H.; Pereira Arias, A. M.; Ackermans, M. T.; Endert, E.; Pijl, H.; Kuipers, F. The effects of carbohydrate variation in isocaloric diet son glycogenolysis and gluconeogenesis in healthy men. *J. Clin. Endocrinol. Metab.* **2000**, *85*, 1963−1967.

(42) Allick, G.; Bisschop, P. H.; Ackermans, M. T.; Endert, E.; Meijer, A. J.; Kuipers, F. A low-carbohydrate/high-fat diet improves glucoregulation in type 2 diabetes mellitus by reducing postabsorptive glycogenolysis. *J. Clin Endocrinol. Metab.* **2004**, *89*, 6193−6197.
(43) Nutall, F. Q.; Ngo, A.; Gannon, M. C. Regulation of hepatic glucose production and the role of gluconeogenesis in humans: is the rate of gluconeogenesis constant? *Diabetes Metab. Res. Rev.* **2008**, *24*, 438−468.
(44) Caperna, T. J.; Shannon, A. E.; Garrett, W. M. A gel-based map of the porcine hepatocyte proteome. *Domestic Anim. Endocrinol.* **2008**, *35*, 142−156.